Registration of Multiple Sensor Earth Science Data

Jacqueline Le Moigne, Jeffrey Morisette,
Peyush Jain
NASA Goddard Space Flight Center
Codes 935 and 586
Greenbelt, MD 20771

Arlene Cole-Rhodes, Kisha Johnson
Electrical &Computer Engineering Dept
Morgan State University
Baltimore, MD 21251

Harold Stone, Ilya Zavorin
UMBC/GEST Center at
NASA Goddard Space Flight Center
Greenbelt, MD 20771

Roger Eastman
Loyola College of Maryland
Baltimore, MD 21210

Nathan Netanyahu
Bar-Ilan University and University of Maryland
College Park, MD 20742

***Abstract*- To address future NASA challenges, integration of multiple source data will be a key component, and as a first step towards this goal, very accurate registration of multi-sensor data is the first requirement for such integration. While navigation often refers to "systematic correction", image registration refers to "precision correction." The systematic correction is model-based, while precision correction is feature-based. Starting from the results of the systematic correction (usually accurate within a few pixels), precision-correction utilizes selected features or control points to refine the geo-location accuracy within one pixel or a sub-pixel. Our work focuses on precision correction or automatic image registration, with the goal of achieving sub-pixel accuracy. We have built a modular registration framework in which different components of the registration process can be assessed and then combined in an optimal manner as a function of the application, the required accuracy and the available computational capabilities.**

I. Introduction

Two of the main goals of NASA mission are "to understand and protect our home planet" and "to explore the universe and search for life." For these two goals, it is very important to understand Earth system processes and to build accurate prediction models. But such an understanding will also be beneficial to NASA's mission to explore the universe by providing knowledge, experience and technology applicable to future observing systems anywhere in the solar system. In addition, future decision support systems, intelligent sensors and adaptive constellations will rely on real- or near-real-time interpretation of Earth observation data, both on-board, in-situ or from ground-based Direct Readout stations. The more expert the system and far-reaching the application, the more important will it be to obtain accurate data.

To address such challenges, integration of multiple sensor data is a key component, and as a first step towards this goal, very accurate registration of multi-sensor data is the first requirement for such integration. Figures 1 and 2 illustrate this scenario for Earth Science and for Exploration planning, where multi-source integration provide improved and more accurate information for either navigation models, prediction models, or planning and decision making systems.

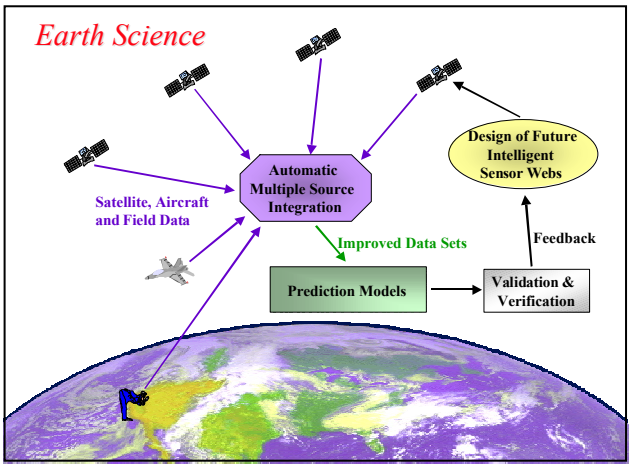

Figure 1
Earth Science Multi-Source Integration

The goal of our project is to develop and assess image registration methodologies that will enable this accurate multi-source integration. While navigation often refers to "systematic correction", image registration refers to "precision correction." The systematic correction is model-based, while precision correction is feature-based. Starting from the results of the systematic correction (usually accurate within a few pixels), precision-correction utilizes selected features or control points to refine the geo-location accuracy within one pixel or a sub-pixel. For many applications, it is very important to reach the sub-pixel accuracy that can be achieved by precision correction. As an example, studies performed on MODIS simulated data have shown that 1 pixel misregistration could imply 50% error in NDVI computation [1]. Our work focuses on precision correction or automatic image registration, with the goal of addressing the three main challenges of image registration:

1. providing methods that can handle mono- and multi-sensor data with multi-resolution from a spatial, spectral or temporal point of view,
2. achieving sub-pixel accuracy,
3. defining reliable accuracy measurements based on:
   - synthetic data
   - manual user registration
   - down-sampled high-resolution data
   - consistency studies.

In our experiments, we assume that the data have already been corrected according to a navigation model and are at a level equivalent to the EOS-level 1B. Assuming that the results of the systematic correction are accurate within a few pixels, our precision-correction algorithms utilize selected image features or control points to refine this geo-location accuracy within one pixel or a sub-pixel. Currently, there is a large quantity of potential image registration methods that have been developed for aerial or medical images and that are applicable to remote sensing images [2,3]. But there is no consolidated approach to select the most appropriate method for a given remote sensing application.

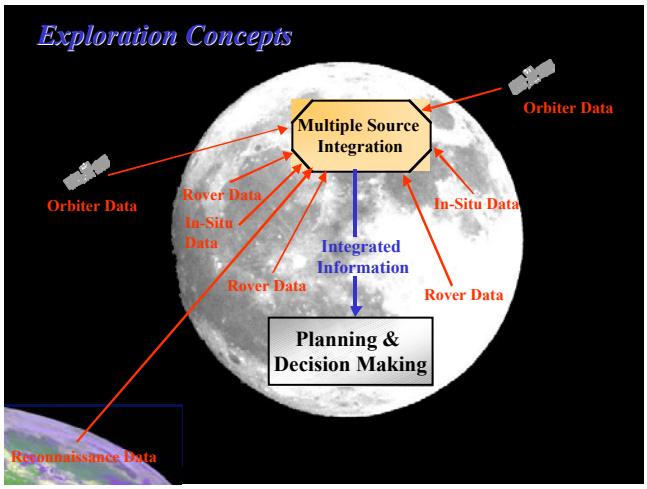

Figure 2
Planning and Decision Making for Planetary Exploration

This paper describes previous and current experiments, and introduces a modular registration framework where various choices for each of these steps can be tested independently. Performance of these algorithms has been evaluated on synthetic data as well as multi-temporal Landsat data and multi-sensor data from several EOS Land Validation Core Sites, including data from the IKONOS, Landsat-7, MODIS, and SeaWIFS sensors. The modular framework and preliminary results are described in section III.

II. Prior Image Registration Experiments

As a general definition, image registration is described as the process that determines the most accurate match between two or more images, and can be defined by three main steps:

1. extraction of features to be used in the matching process,
2. feature matching strategy and metrics,
3. resampling or indexing of the data.

Many choices are available for each of the previous three steps. In earlier work, we investigated step (1), first focusing on correlation-based methods, then looking at optimization-based methods.

(A) Correlation-Based Experiments

Using correlation as a similarity metrics, our first experiments focused on features assessment, This work showed that, as expected, edges or edge-like features like wavelets are more robust to noise and local intensity variations. Wavelet features that are considered as potential registration features are either low-pass features, which provide a compressed version of the original data and some texture information, or high-pass features, which provide detailed edge-like information, Comparing edges and wavelets, we observed that orthogonal wavelet-based registration was usually faster although not always as accurate than a full-resolution edge-based registration [4]. This was obtained by exploiting the multi-resolution nature of wavelets, where an approximation of the transformation is computed at very low-spatial resolution, and then iteratively refined at higher and higher resolutions. But because of this decimation, orthogonal wavelets lose the invariance to translation since features can migrate between frequency subbands. By lack of translation (resp. rotation) invariance, we mean that the wavelet transform does not commute with the translation (resp. rotation) operator. To study the effects of translation, we conducted a first study [5] that quantitatively assessed the use of orthogonal wavelet sub-bands as a function of features' sizes. The results showed that high-pass sub-bands are more sensitive to translation than low-pass sub-bands which are relatively insensitive provided that the features of interest have an extent at least twice the size of the wavelet filters. A second study [6] investigated the use of an overcomplete frame representation, the "Steerable Pyramid" [7]. It was shown that, as expected and due to their translation- and rotation- invariance, Simoncelli's steerable filters perform better than Daubechies' filters. Rotation errors obtained with steerable filters were minimum, independent of rotation size or noise amount. Noise studies also reinforced the results that steerable filters show a better robustness to larger amounts of noise than do orthogonal filters. Another result of this study is that Simoncelli band-pass features are more robust, but less accurate than low-pass features.

(B) Optimization-Based Experiments

This earlier work focusing on correlation-based methods used exhaustive search. One of the main drawbacks of this method is the prohibitive computation times when the number of transformation parameters increases (e.g., affine transformation vs. shift-only), or when the size of the data increases (full size scenes vs. small portions, multi-band

processing vs. mono-band). To answer this concern, we looked at different features using an optimization-based method.

In these experiments, we chose an optimization based on a gradient descent method and using an L2 norm as similarity metrics. Using this matching methodology, we compared features obtained from two different multi-resolution decompositions, the Simoncelli steerable pyramid and the Spline decompositon [8]. While the Simoncelli steerable pyramid produces low-pass and band-pass features, the Spline pyramid only produces low-pass features. Results then showed than for a gradient optimization matching, Simoncelli/low-pass features have a better radius of convergence, while Simoncelli/band-pass features are the best in terms of accuracy and consistency, but than when they converge, the Spline features present the best accuracy.

(C) Similarity Measures Experiments

Using Simoncelli band-pass features as registration features, exhaustive search as well as a stochastic gradient optimization matching strategy (Spall's algorithm [10]) were utilized to compare 2 similarity measures: correlation and mutual information [9]. The results show that similarity peaks obtained with mutual information are sharper than those obtained with correlation; this can be important when we need to reach sub-pixel registration accuracy. Furthermore, when using mutual information with a stochastic gradient, results show an accuracy of 0.01 pixel on synthetic test data, 0.64 pixel on multi-temporal (cloudy) data, and 0.34 pixel on multi-sensor data.

Following these preliminary experiments focusing on one or another of the components of the registration process, the next step is then to perform systematic comparisons, where all the registration components can be combined in different ways and assessed on well-chosen test data.

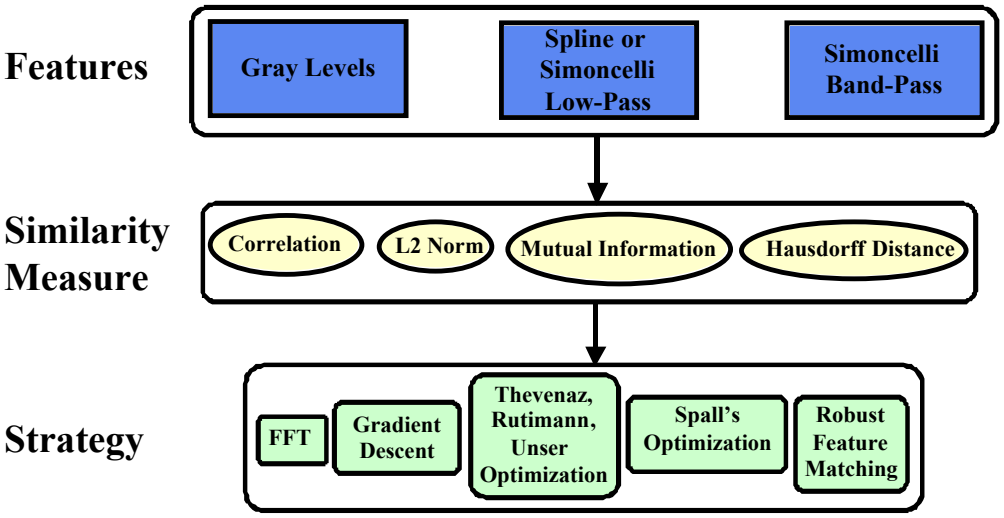

Figure 3

Modular Approach to Image Registration Combining Various Choices for Feature Extraction, Similarity Metrics and Matching Strategy

III. A MODULAR IMAGE REGISTRATION FRAMEWORK

In order to perform these systematic studies and to enable new components to be tested in a rigorous fashion, we started building a modular image registration framework. The concept guiding this framework is that various components of the registration process can be combined in several ways in order to reach optimum registration on a given type of data and under given circumstances. Thereby, the purpose of this framework is double-fold:

1. it represents a testing framework to:
    a. Assess various combinations of components as a function of the applications,
    b. Assess a new registration component compared to other known ones.
2. it is be the basis of a registration tool where a user can "schedule" a combination of components as a function of the application at hand, the available computational resources and the required registration accuracy.

Figure 3 illustrates this concept, where a registration algorithm is defined as the combination of a set of features, a similarity measure, and a matching strategy. In our current framework:

- features can be either gray levels, Low-Pass features from Simoncelli steerable filters decomposition or from a Spline decomposition, or Simoncelli Band-Pass features,
- similarity metrics can be either cross-correlation, the L2 Norm, Mutual Information or an Hausdorff distance,
- matching strategies are either based on a Fast Fourier Correlation, three different types of optimization - pure gradient descent, a Marquard-Levenberg approach (developed by Thevenaz et al [10], denoted TRU in the

remaining of this paper) or a stocchastic gradient approach (developed by Spall et al) [9], and a Robust Feature Matching approach [11].

An early set of these combination algorithms was tested on three different datasets, using transformations composed of a rotation, a translation and an isometric scaling (i.e., scale factor similar in both x- and y-directions. By combining these different components, five algorithms were developed:

- Method 1: Gray Levels matched by Fast Fourier Correlation [12].
- Method 2: Gray Levels matched by gradient descent [13] using a least squares criterion.
- Method 3: Spline or Simoncelli (Band- or Low-Pass) Pyramid features matched by optimization using "TRU" [14].
- Method 4: Simoncelli wavelet features matched by optimization of the mutual information criterion using Spall algorithm [9].
- Method 5: Simoncelli wavelet features using a robust feature matching algorithm and a generalized Hausdorff distance [11,15].

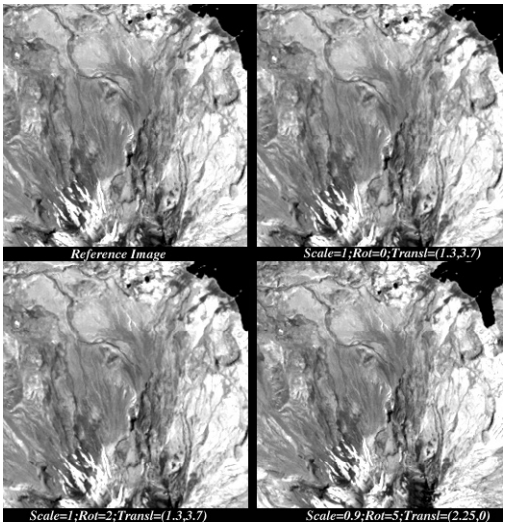

Figure 4 - ***Synthetic Test Data***
Reference Image and 3 Transformed Input Images

For some of the methods (1 and 5), registration is computed on individual sub-images and then integrated by computing a global transformation, for the others (2-4), registration is computed on the entire images but iteratively, using the pyramid decompositions.

Three different datasets were utilized for the study.

(A) Synthethic Dataset Experiments

The first dataset is synthetically created using a 512x512 section of a Landsat-TM (band 4) of a Pacific Northwest scene. This reference image is transformed using the combination of a scaling, a rotation and a translation. Figure 4 shows the reference data with three examples of transformed images. Both rotation and scaling are done with respect to the center of the image. For this study, no noise is added to the dataset, After the transformation is applied, the 256x256 centers of the transformed images are extracted and registered to the 256x256 center of the original reference image. Seven different transformed images have been created using scales in the range [0.9, 1.1], rotations varying between 0 and 3 degrees, and translations between 0 and 4 pixels in each direction. Table 1 shows the results of 4 of the algorithms (Methods 1,2,3,4) applied on this dataset. We can notice that most results are within at most 1/3 pixel of the "truth transformation."

Synthetic Data wrt r256	Method 1 Fast Correl	Method 3a TRU/Spline	Method 3b TRU/SimB	Method 3c TRU/SimL	Method 4 MI/Spall
r256					
Scale	1.0000	1.0000	1.0000	1.0000	1.0001
Rotation	0.0000	0.0000	0.0000	0.0000	0.0122
Shift-x	0.0000	0.0000	0.0000	0.0000	-0.0098
Shift-y	0.0000	0.0000	0.0000	0.0000	-0.0108
i256_r2					
Scale	0.9998	0.0000	0.9999	0.9999	1.0001
Rotation	1.9922	2.0001	1.9977	1.9977	2.0820
Shift-x	-0.0723	0.0007	-0.0002	-0.0002	-0.0070
Shift-y	0.0662	0.0005	-0.0001	-0.0012	0.0278
i256_tx1.3_ty3.7					
scale	0.9997	1.0000	0.9994	1.0000	1.0000
Rotation	-0.0294	-0.0003	-0.0019	-0.0006	0.0011
Shift-x	1.0131	1.3001	1.2953	1.2996	3.7071
Shift-y	3.9321	3.6983	3.6955	3.6996	1.2908
i256_sc1.1					
Scale	1.0996	1.1000	1.0999	1.1000	1.0999
Rotation	-0.0001	0.0002	0.0000	-0.0003	0.0049
Shift-x	0.0002	0.0004	-0.0011	0.0001	-0.0117
Shift-y	0.0005	-0.0001	0.0043	-0.0001	0.0112
i256_sc0.9					
Scale	0.9014	0.9000	0.9001	0.9000	0.9001
Rotation	-0.0392	0.0000	0.0005	0.0000	0.0080
Shift-x	0.0000	-0.0002	0.0002	0.0003	-0.0251
Shift-y	-0.0003	-0.0005	-0.0022	-0.0013	-0.0099
i256_r2_tx1.3_ty3.7					
Scale	1.0001	1.0000	1.0000	1.0000	1.0000
Rotation	2.0131	2.0002	1.9992	2.0000	2.0004
Shift-x	1.2172	1.3001	1.2981	1.3009	1.3049
Shift-y	3.7748	3.6997	3.6950	3.7027	3.7052
i256_sc0.9_r5_tx2.25					
Scale	0.9018	0.9000	0.9616	0.8999	0.9000
Rotation	4.9566	4.9996	3.8120	4.9991	5.0080
Shift-x	2.2876	2.2505	-4.3352	2.2513	2.2517
Shift-y	0.3609	-0.0014	4.7762	-0.0026	0.0034
56_sc1.1_r3_tx3.1_ty2.75					
Scale	1.1002	1.1000	1.0632	1.1000	1.1000
Rotation	2.9922	3.0001	-3.0035	3.0002	2.9981
Shift-x	2.7988	3.1000	-3.2838	3.1002	3.0782
Shift-y	2.6428	2.7500	-8.8802	2.7503	2.7507

Table 1 - ***Rsults of 7 Algorithms on Synthetic Data***

(B) Multi-Temporal Dataset Experiments

The multi-temporal dataset has been acquired over two areas, Central Virginia and the Washington DC/Baltimore area. For each area, one reference scene is chosen and 6 to 8 reference chips (of size (256x256) are extracted. Also for each area, the dataset includes 4 input scenes known from their UTM (Universal Transverse Mercator projection) coordinates. From these coordinates, windows corresponding to each reference chip of that area are computed and extracted, and local chip/window registrations are performed using a robust feature matching method with a partial Hausdorff distance applied to Simoncelli/band-pass features [15]. Figure 5 shows a few examples of chip/window pairs. Then, for each pair of scenes, a global registration is being computed with a generalized Least Mean Squares method that combines all previous local registrations. Compared to manual registration, these multi-temporal experiments

produced registration accuracies included between 0.21 and 0.59 pixel.

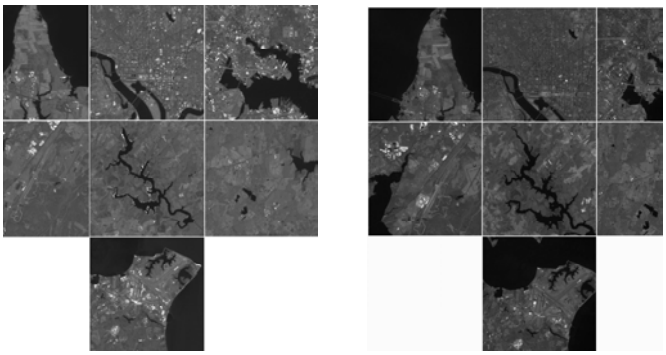

Figure 5
Examples of Chip/Window Pairs for the DC/Baltimore Area

(C) Multi-Sensor Dataset Experiments

The third dataset used in this study represents multi-sensor data acquired by two different sensors over four of the MODIS Validation Core Sites. The four sites represent four different types of terrain in the United States:

- Coast Reserve area with the Virgina site, data acquired in October 2001.
- Agricultural area with the Konza Prairie in the state of Kansas, data acquired July to August 2001.
- Mountainous area with the CASCADES site, data acquired in September 2000.
- Urban area with the USDA, Greenbelt, Maryland, site, data acquired in May 2001.

Figures 6 and 7 show examples of these data.

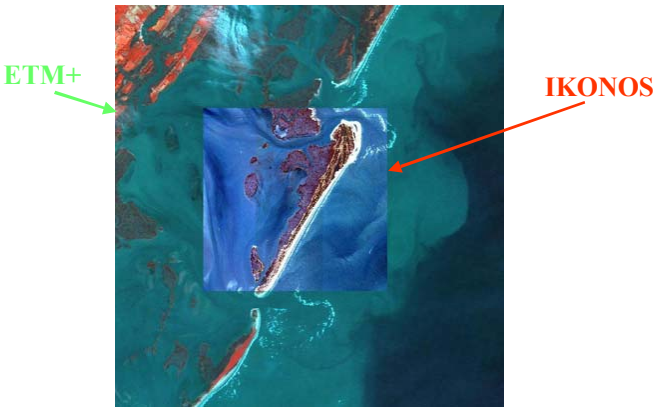

Figure 6
ETM and IKONOS data of the Virginia Coastal Area

The two sensors and their respective bands and spatial resolutions involved in this study are:

1. IKONOS Bands 3 (Red) and 4 (Near-Infrared), spatial resolution of 4 meters per pixel,
2. Landsat-7/ETM+ Bands 3 (Red) and 4 (Near-Infrared), spatial resolution of 30 meters per pixel.

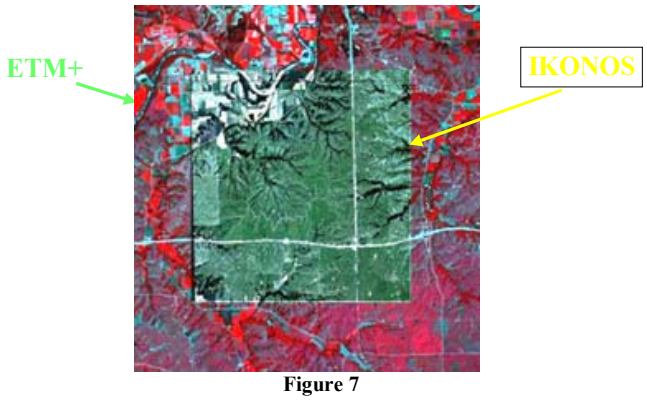

Figure 7
ETM and IKONOS data of the CASCADES Mountainous Area

(Future multi-sensor studies on the same sites will also involve MODIS and SeaWIFS data). In this study, wavelet decomposition was utilized not only to compute registration features, but also to bring various spatial resolution data to similar resolutions, by performing recursive decimation by 2. For example, after 3 levels of wavelet decomposition, the IKONOS spatial resolution is brought to 32 meters that, compared to the Landsat spatial resolution, corresponds to a scaling of 1.07. This will be the scaling expected when registering IKONOS to Landsat data in our study. Overall, for each site, five different registrations are performed and results are shown in Tables 2 for two of the sites, Virginia-Coast and Cascades-Mountainous, and for Methods 1 to 4.

VA_Coast	Method 1 Fast Correl	Method 2 Grad Desc	Method 3a TRU/Spline	Method 3b TRU/SimB	Method 3c TRU/SimL	Method 4 MI/Spall
IKONOS/Red-IKONOS/NIR						
Scale	1.0000	1.0000	1.0000	0.9999	1.0000	1.0006
Rotation	-0.0008	0.0282	-0.0005	0.0017	-0.0002	0.0811
Shift-x	0.0072	-1.5474	-0.1644	0.0523	-0.2421	0.9223
Shift-y	-0.0542	1.6686	-0.4944	-0.5597	-0.5315	0.7505
IKONOS/Red-ETM/Red						
Scale	1.0661	1.0638	1.0662	1.6094	1.0669	1.0661
Rotation	0.0013	0.1531	0.0204	-1.3397	0.0568	0.1040
Shift-x	12.8575	12.7673	12.9748	-105.3350	12.9902	13.0244
Shift-y	13.1722	12.4212	13.2198	83.6175	13.3562	14.1378
IKONOS/Red-ETM/NIR						
Scale	1.0619	1.0893	1.0515	1.5185	3.0250	1.0664
Rotation	-0.1210	0.6965	1.5185	7.5141	6.6137	0.0103
Shift-x	12.3951	13.5345	10.6674	-45.6183	-205.4730	12.2158
Shift-y	12.2179	13.4872	9.3905	69.9682	248.2180	13.1563
IKONOS/NIR-ETM/Red						
Scale	1.0610	1.0679	1.0564	0.9886	1.0516	1.0674
Rotation	-0.9030	2.1602	-1.0406	-0.5544	-1.1490	0.9718
Shift-x	10.3298	19.3508	27.7790	-1.5585	28.2731	16.0900
Shift-y	11.5491	17.7127	6.6591	-1.7722	6.5726	16.0972
IKONOS/NIR-ETM/NIR						
Scale	1.0654	1.0681	1.0651	1.4050	1.0668	1.0663
Rotation	-0.1093	0.0435	0.0111	3.7209	0.0375	0.0063
Shift-x	12.5909	12.1728	13.0008	-38.6769	12.9493	12.8556
Shift-y	12.8984	12.4887	13.1058	2.5245	13.2238	13.2462
ETM/Red-ETM/NIR						
Scale	1.0000	0.9960	0.9998	0.9998	0.9997	1.0001
Rotation	0.0015	0.1464	-0.0146	-0.0136	-0.0214	-0.0020
Shift-x	-0.0670	-2.3708	-0.2048	-0.2107	-0.2243	0.8507
Shift-y	-0.0136	-24.6208	-0.4854	-0.5024	-0.6841	0.6654

Table 2a - ***Results of 6 algorithms on the Virginia-Coast Area***

For this study, no exact ground truth is available, but we expect the multi-modal intra-sensor registrations to be scale=1, rotation=0, translation=(0,0), and we expect a scale=1.07 for the IKONOS to Landsat registrations. The results of Tables 2 show that, as expected the registrations based on gray levels are less reliable on inter-band registrations than those based on edge-like features, but, when reliable, these results are more accurate. Also, since no ground truth was available for this dataset, consistency between algorithms was measured: we observed that most results were within 1/4 to 1/3 pixel of each other. Self-

consistency of 2 of the methods was also checked, by performing circular registrations: for example if 3 images A, B, and C are considered, registrations of pairs (A,B), (B,C) and (A,C) are compared. In this experiment, we observed that the tested algorithms were self-consistent within 1/8 pixel.

CASCADES_Mountains	Method 1 Fast Correl	Method 2 Grad Desc	Method 3a TRU/Spline	Method 3b TRU/SimB	Method 3c TRU/SimL	Method 4 MI/Spall
IKONOS/Red-IKONOS/NIR						
Scale	1.0000	1.0000	1.0000	1.0001	1.0000	1.0003
Rotation	0.0003	0.1580	0.0006	0.0009	0.0009	0.0177
Shift-x	0.0135	0.0025	-0.0240	-0.0362	-0.0464	0.0204
Shift-y	0.0135	-0.0001	-0.1603	-0.1827	-0.2090	0.0535
IKONOS/Red-ETM/Red						
Scale	1.0644	1.0621	1.1006	1.0642	1.0646	1.0645
Rotation	0.0917	0.1137	-0.0500	0.0760	0.0703	0.1302
Shift-x	8.6744	8.1151	11.4319	8.6515	8.6323	8.7768
Shift-y	10.1616	9.2868	12.3680	10.0627	10.0836	10.0392
IKONOS/Red-ETM/NIR						
Scale	1.0651	1.0641	0.9962	1.0649	1.0000	1.0640
Rotation	0.0883	0.1349	-0.0316	0.0878	0.0000	0.1138
Shift-x	8.6944	8.1211	0.0321	8.6573	0.0000	8.8979
Shift-y	10.2174	9.5540	0.2538	10.1193	0.0000	10.2239
IKONOS/NIR-ETM/Red						
Scale	1.0641	1.0630	1.0765	1.0646	1.0981	1.0656
Rotation	0.0390	0.2133	-0.5836	0.0807	0.0694	0.1277
Shift-x	8.5615	7.9878	10.5558	8.5537	11.9510	8.7318
Shift-y	10.1641	9.5301	9.9043	10.1538	8.3562	9.9239
IKONOS/NIR-ETM/NIR						
Scale	1.0647	1.0643	1.0649	1.0649	1.0648	1.0652
Rotation	0.1086	0.1024	0.0725	0.0714	0.0683	0.1096
Shift-x	8.6681	8.1394	8.7279	8.7094	8.6437	8.6629
Shift-y	10.1669	9.5819	10.1404	10.1394	10.1489	10.1561
ETM/Red-ETM/NIR						
Scale	1.0000	0.9615	1.0000	1.0001	1.0000	1.0000
Rotation	-0.0006	1.3168	-0.0079	-0.0087	-0.0085	0.0929
Shift-x	0.0793	4.7291	-0.1191	-0.1415	-0.0995	0.7340
Shift-y	-0.0290	10.1447	-0.1663	-0.2173	-0.1334	0.9420

Table 2b - ***Results of 6 algorithms on the Cascades-Mountainous Area***

V. Conclusion And Future Work

The study presented in this paper deals with multi-sensor multi-resolution precision correction or image registration. Using gray levels or wavelet features, several similarity metrics and search strategies were being tested using synthetic data as well as IKONOS versus Landsat data over four well-chosen EOS Land Validation Core Sites.

Current and future work will involve a systematic study involving:

- all possible combinations of components to form the algorithms and their application to all datasets,
- an extended synthetic dataset with noise added, radiometric transformation applied, and systematic transformations in well-chosen ranges of rotations, translations and scaling.
- a larger number of sensors for multi-sensor data registration.
- potentially, the application of this framework to the registration of MARS data.

From all these tests, we will be able to categorize the different algorithms in terms of their accuracy but also in terms of their sensitivity to initial (i.e., navigation) conditions, their computational and memory requirements, and as well as their implementations on high-performance and reconfigurable implementations.

Results of this study will be useful for 2 different purposes: (1) provide automatic quality assessment of the geo-location of remote sensing data by performing inter-algorithm consistency studies; (2) be the foundations for the design of future on-board applications and potentially planetary exploration.

Acknowledgements

The authors wish to acknowledge the support of the NASA Intelligent Systems/ Intelligent Data Understanding Program.

VI. References

[1] J. R. Townshend, C.O. Justice, J. McManus, "The Impact of Misregistration on Change Detection," IEEE Transactions on Geoscience and Remote Sensing, Vol. 30, No. 5, 1992.

[2] L. Brown, "A Survey of Image Registration Techniques," *ACM Computing Surveys*, vol. 24, no.4, 1992.

[3] J. Le Moigne, W.J. Campbell, and R.F. Cromp, 2002, "An Automated Parallel Image Registration Technique of Multiple Source Remote Sensing Data," *IEEE Transactions on Geoscience and Remote Sensing*, Vol. 40, No. 8, pp. 1849-1864, August 2002.

[4] J. Le Moigne, W. Xia, J. Tilton, T. El-Ghazawi, M. Mareboyana, N. Netanyahu, W. Campbell, R. Cromp, "First Evaluation of Automatic Image Registation Methods," International Geoscience and Remote Sensing Symposium, *IGARSS'98*, Seattle, WA, July 1998.

[5] H.S. Stone, J. Le Moigne, and M. McGuire, "Image Registration Using Wavelet Techniques," IEEE Transactions on Pattern Analysis and Machine Intelligence, Vol. 21, No. 10, Oct. 1999.

[6] J. Le Moigne, and I. Zavorin, "Use of wavelets for image registration," 2000 SPIE Aerosense Conference, Wavelet Applications, Orlando, Florida, April 2000.

[7] E. Simoncelli, W. Freeman, "The Steerable Pyramid: A Flexible Architecture for Multi-Scale Derivative Computation," *2-nd IEEE International Conference on Image Processing,* 1995.

[8] I. Zavorin H. Stone and J. Le Moigne, "Evaluating Performance of Automatic Techniques for Sub-Pixel Registration of Remotely Sensed Imagery," SPIE Electronic Imaging 2003, Image Processing: Algorithms and Systems II Conference, Santa Clara, January 2003.

[9] A. Cole-Rhodes, K. Johnson, J. Le Moigne, and I. Zavorin, 2003, "Multiresolution Registration of Remote Sensing Imagery by Optimization of Mutual Information Using a Stocchastic Gradient," IEEE Transactions on Image Processing, Vol. 12, No. 12, pp. 1495-1511, December 2003.

[10] P. Thévenaz, U. Ruttimann, and M. Unser, "A pyramid approach to subpixel registration based on intensity", IEEE Transactions on Image Processing, Vol. 7, No. 1, 1998.

[11] D.M. Mount, N.S. Netanyahu, J. Le Moigne, "Efficient Algorithms for Robust Feature Matching," Special Issue Pattern Recognition Image Registration, Vol. 32, No. 1, pps.17-38, January 1999.

[12] H.S. Stone, "Progressive Wavelet Correlation Using Fourier Methods," IEEE Transactions on Signal Processing, Vol. 47, No. 1, 97-107, 1999.

[13] R. Eastman, and J. Le Moigne, "Gradient-Descent Techniques for Multi-Temporal and Multi-Sensor Image Registration of Remotely Sensed Imagery," in FUSION'2001, 4-th Int. Conf. Info. Fusion, CA, August 2001.

[14] I. Zavorin, and J. Le Moigne, 2004, "On the Use of Wavelets for Image Registration," provisionnally accepted for IEEE Transactions on Image Processing, October 2003.

[15] N. Netanyahu, J. Le Moigne, J. Masek, "Geo-Registration of Landsat Data by Robust Matching of Wavelet Features," to appear in IEEE Transactions on Geoscience and Remote Sensing, 2004.